Letter

Electronic structure of the putative room-temperature superconductor $Pb_9Cu(PO_4)_6O$

Liang Si[1,2,*] and Karsten Held[2,†]

[1]*School of Physics, Northwest University, Xi'an 710127, China*
[2]*Institute of Solid State Physics, TU Wien, 1040 Vienna, Austria*

(Received 1 August 2023; revised 6 September 2023; accepted 7 September 2023; published 20 September 2023)

A recent paper [Lee *et al.*, J. Kor. Cryst. Growth Cryst. Technol. **33**, 61 (2023)] provides some experimental indications that $Pb_{10-x}Cu_x(PO_4)_6O$ with $x \approx 1$, coined LK-99, might be a room-temperature superconductor at ambient pressure. Our density-functional theory (DFT) calculations show lattice parameters and a volume contraction with x, very similar to experiment. The DFT electronic structure shows Cu^{2+} in a $3d^9$ configuration with two flat Cu bands crossing the Fermi energy. This puts $Pb_9Cu(PO_4)_6O$ in an ultracorrelated regime and suggests that, without doping, it is a Mott or charge-transfer insulator. If doped, such an electronic structure might support flat-band superconductivity or a correlation-enhanced electron-phonon mechanism, whereas a diamagnet without superconductivity appears to be rather at odds with our results.

DOI: 10.1103/PhysRevB.108.L121110

Hitherto, milestones of superconductivity research include its discovery by Onnes in 1911, the BCS theory of Bardeen, Cooper and Schrieffer [1], the discovery of high-temperature superconductors by Bednorz and Müller [2], and, more recently, that of hydride superconductors by Eremets and co-workers [3] as well as nickelate superconductivity by Li *et al.* [4–6]. Ever since Onnes' discovery, finding a room-temperature superconductor has been *the* big dream of condensed-matter physics. Such a superconductor would revolutionize the way we generate, transport, and consume electric energy.

Lee *et al.* [7–9] proclaim that they have successfully synthesized such a room-temperature superconductor, $Pb_{10-x}Cu_x(PO_4)_6O$ with $0.9 < x < 1$, even at ambient pressure. This is indicated by (i) a drastic drop in the resistivity [7,9] (according to [8] to the order of 10^{-10}–10^{-11} $\Omega\,$cm despite a quite substantial noise level [7,9]); (ii) a negative (diamagnetic) susceptibility and levitation of the superconductor on a magnet [9]; and (iii) extraordinarily sharp voltage jumps at the critical currents [7,8] with a vanishing critical current strength at temperatures of about 400 K and fields of about 3000 Oe [8]. The recipe to synthesize $Pb_{10-x}Cu_x(PO_4)_6O$ appears easy enough [9] for other groups to follow suit. Thus further experiments will reveal whether $Pb_9Cu(PO_4)_6O$ is indeed the first room-temperature superconductor or not.

In any case, the experiments by Lee *et al.* [7–9] are exciting and definitely call for a more thorough theoretical understanding of this rather unusual material. The crystal structure of $Pb_9Cu(PO_4)_6O$ as obtained by x-ray diffraction (XRD) [7–9] is a modified lead-apatite structure and is shown in Fig. 1. The first step to obtain a theoretical understanding of a new material is an impartial density-functional theory (DFT) calculation.

In this paper, we perform such DFT calculations, focusing on the crystal and electronic structure. The latter can serve at least as a starting point for subsequent many-body calculations. Relaxing the lead-apatite crystal structure, we find very similar lattice parameters to those of Lee *et al.* [7,9]. The calculation further confirms the observed lattice compression when substituting Pb by Cu. The DFT electronic structure of the parent compound ($x = 0$) is insulating, whereas there are two very flat predominately Cu d-bands crossing the Fermi energy for $x = 1$. These flat bands are prone to be split into Hubbard bands. In this case, undoped $Pb_9Cu(PO_4)_6O$ would become a Mott or charge-transfer insulator, depending on the relative position of the lower Hubbard band and the other bands.

Computational method. For the DFT structural relaxations and electronic structure calculations, we use VASP [10,11] (projected augmented plane waves) with the GGA-PBESol [12] exchange-correlation potential. More details are available Sec. I in the Supplemental Material [13].

Crystal structure. Let us start with the undoped parent compound $Pb_{10}(PO_4)_6O$, a lead apatite with a hexagonal structure ($P6_3/m$, 176) identical to that displayed in Fig. 1 [14]. For the parent compound, there is still the uncertainty at which position (out of four) the one oxygen is to be placed: open circles or the dark red circles at the edge(s) of Fig. 1(a). Here, we refer to this O as the "extra O," as it is not part of the six PO_4 tetrahedra. For a single unit cell, however, all of these O positions are equivalent. We have relaxed the structure in DFT and find lattice parameters in Table I to agree with experiment. We have further checked all possible distributions of four O's in the larger supercell of Fig. 1(b) consisting of four formula

---

[*] liang.si@ifp.tuwien.ac.at
[†] held@ifp.tuwien.ac.at

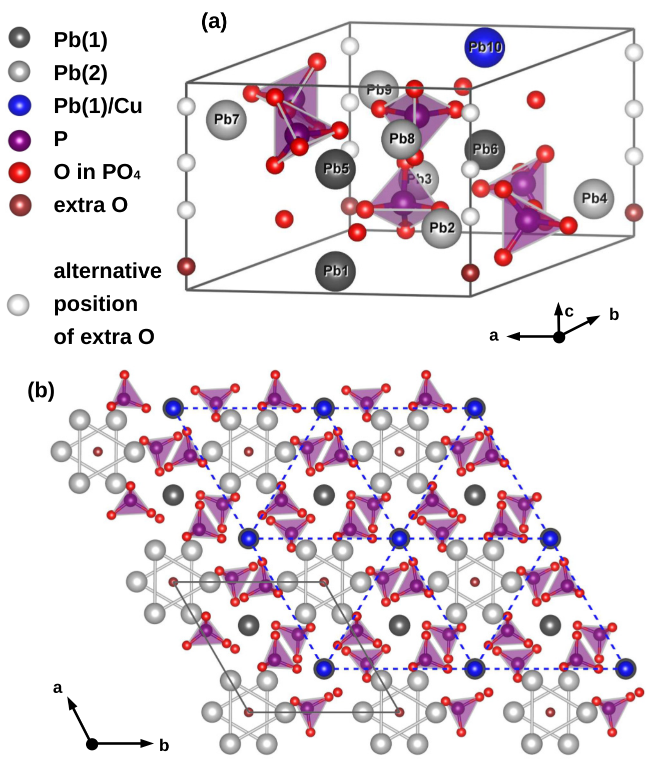

FIG. 1. Crystal structure of $Pb_9Cu(PO_4)_6O$: (a) single unit cell in side view; (b) four unit cells plus surrounding atoms in top view. There is some uncertainty regarding the position of the one extra O per formula unit and at which Pb site Cu is substituted. The extra O can occupy the dark red position as indicated in (a) or one of the empty white circles instead. As for the 10 Pb atoms in the unit cell, these fall into two symmetry classes: Pb(1) (dark gray) and Pb(2) (light gray). The latter are located around the extra O; see (b). Our DFT calculations show that it is, however, energetically favorable for the Cu atom to be as far away from the extra O as possible, i.e., to occupy the blue Pb10 position of the Pb(2) class. This leaves us—for a lead-apatite structure and a single formula unit as the unit cell—with the structure displayed.

units; see Sec. I in the Supplemental Material [13]. The energy difference between the different oxygen arrangements is only ~6 meV per unit cell, which corresponds to 70 K and is hence not relevant at room temperature.

Next we study the crystal structure of the putative superconductor $Pb_9Cu(PO_4)_6O$. The XRD data of *Lee et al.* [7–9] show a modified lead-apatite structure. In one unit cell of this structure, there are 4 × 10 different arrangements of the extra O and doped Cu, some of them related by symmetry. We have calculated all possibilities (see Sec. I in the Supplemental Material [13]), and we find that Cu prefers to occupy the position that is farthest away from O [8,9]. This results in the supercell displayed in Fig. 1(a) with Cu occupying one of the four dark gray/blue Pb(1) sites. The energy gain compared to other Cu-O arrangements is at least 12.1 meV; see Sec. I B in the Supplemental Material [13].

TABLE I. DFT relaxed lattice parameters and unit cell volume compared to experiment.

Phase	a (Å)	c (Å)	V (Å^3)	From
$Pb_{10}(PO_4)_6O$	9.865	7.431	626.28	expt. [7,9]
$Pb_{10}(PO_4)_6O$	9.825	7.371	616.22	this work (GGA-PS)
$Pb_9Cu(PO_4)_6O$	9.843	7.428	623.24	expt. [7,9]
$Pb_9Cu(PO_4)_6O$	9.661	7.226	584.04	this work (GGA-PS)

Indeed, it was already discussed in [7–9] that the six Pb sites around the tube where the extra O is located [light gray Pb(2) sites in Fig. 1] are not substituted with Cu, that Cu instead occupies one of the dark gray sites [Pd(1)] further away from the extra O in agreement with our DFT calculation. Our DFT crystal structure also confirms the volume reduction compared to the parent compound, see Table I, albeit it is considerably larger in DFT than in experiment.

The periodic continuation of the single unit cell is shown in the the top view of Fig. 1(b). Here, the Cu atoms (blue) are arranged in a two-dimensional triangular lattice and the Pb(1) atoms (dark gray) in a similar triangular lattice in essentially the same layer; see Fig. 1(b). In the c direction, this is interlaced by a similar layer of only Pb(1) atoms that sit exactly beneath the first layer and are thus not visible in Fig. 1(b). The Pb(2) atoms (light gray) are arranged instead in a hexagon (two triangles in different layers) around the position (channel) of the extra O. We cannot exclude a more complex long-range arrangement of the Cu and extra O sites based on a larger unit cell at the moment. While this can change the lattice of the Cu sites substantially, the main findings presented in the Conclusion are not affected.

Electronic structure. Figure 2(a) shows the calculated band structure of the parent compound and that of the putative superconductor. In agreement with experiment [9], the parent compound is insulating with a rather large gap of 2.3 eV between the O-p and Pb-p states in DFT (see Sec. II in the Supplemental Material for the detailed DOS). Note that this gap may even be underestimated in DFT because for sp materials the nonlocal exchange tends to further separate occupied from unoccupied states and thus to increase the band gap.

When substituting one Pb by Cu, two flat bands cross the Fermi energy, labeled “1” and “2” in Fig. 2(c). The charge distribution of these flat bands in Fig. 2(d) reveals that they originate from the Cu orbitals but with a very strong hybridization to oxygen. These two narrow bands are occupied by three electrons per unit cell. Copper is thus essentially in an effective Cu^{2+} state with a $3d^9$ electronic configuration.

Due to the large Cu-Cu distance (≈10 Å) in the lead-apatite structure, the Cu-Cu hopping is extremely small, which explains that these bands are so narrow. For example, the bandwidth of the conduction band near the Fermi energy is only ≈120 meV. The small hopping certainly also contributes to the experimental observation that the high-temperature metallic phase is a very bad metal with a large resistivity of 0.02 Ω cm at temperatures $T \gtrsim 380$ K [7,9].

Figure 3 shows the total as well as the partial-Cu DOS around the Fermi energy. The other partial DOSs can be found in Sec. II in the Supplemental Material [13]. The flat bands are reflected by a narrow peak of the DOS at the Fermi energy of predominately Cu-d character but also with a sizable oxygen intermixing; the DOS at −0.4 eV originates from

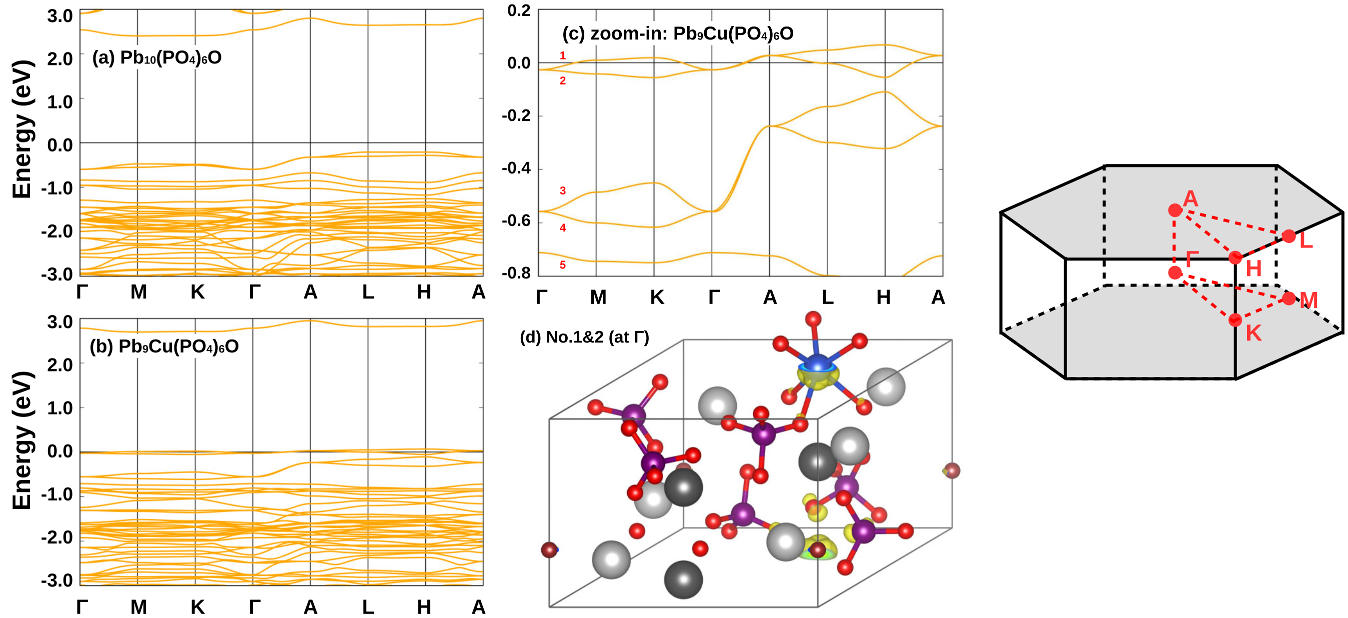

FIG. 2. DFT band structure of $Pb_{10-x}Cu_x(PO_4)_6O$: (a) parent compound at $x = 0$; (b) putative superconductor at $x = 1$; and (c) zoom-in of (b). The Fermi energy is set to zero. The top-right panel shows the high-symmetry k-points selected for plotting the band structure in (a)–(c). Panel (d) shows the band decomposed charge-density distribution (at $k = \Gamma$) of the two bands crossing the Fermi energy: No. 1 and No. 2 index the bands in (c) by their energy below the Fermi energy.

the two somewhat more dispersive bands below the Fermi surface [labeled 3 and 4 in Fig. 2(c)] and predominately from the extra oxygen now with some Cu admixture; see partial DOSs and charge distribution in Sec. II in the supplemental material [13].

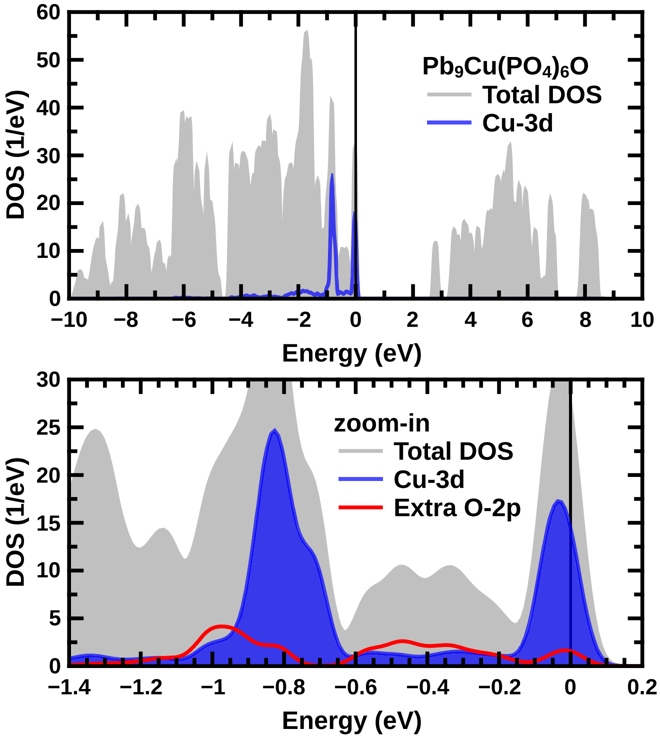

FIG. 3. DFT total DOS and that of Cu-3d and (extra) O-2p (atomically and orbitally resolved) for $Pb_9Cu(PO_4)_6O$. Lower panel: zoom-in. For the other partial DOSs, see Sec. II in the Supplemental Material [13].

Discussion: Effects of electronic correlations. The low-energy electronic degrees of freedom are dominated by the two flat Cu d-bands crossing the Fermi energy, with a bandwidth of only 120 meV (or hoppings t of the order of 10 meV). The local Cu d-d interaction will be much larger. We can expect it to be similar to that of cuprate superconductors, with a similar $3d^9$ configuration, and $U \approx 3$ eV [15,16]. If two (instead of one) low-energy Cu d-orbitals are relevant, U would be even higher because both orbitals still participate in the screening. On the other hand, the strong oxygen intermixture to this band can also reduce the Coulomb interaction. In any case, this puts these two flat bands of $Pb_9Cu(PO_4)_6O$ in an ultra-correlated regime. With $U/W \approx 25$ and for integer filling, the two flat bands can be expected to be split into Hubbard bands if electronic correlations are included in, e.g., DFT+dynamical mean-field theory [17,18]. Let us emphasize that this conclusion as well as that of a fully spin-polarized DFT+U magnetic state in Sec. III in the Supplemental Material [13] does not depend on the precise value of U; U would need to be an order of magnitude smaller to obtain a metal.

This suggests that at least a slight doping is required to arrive at a metallic system as observed in experiment [7–9]. It would put such a doped $Pb_{10-x}Cu_x(PO_4)_6O$ compound into the category of a doped Mott or charge-transfer insulator. In such a situation, we can expect a very large quasiparticle renormalization of the DFT DOS at the Fermi surface. This will further reduce the width of the flat Cu bands. Also the experimentally observed large resistivity of the metallic phase corroborates this picture.

While we can definitely say that the low-energy physics of $Pb_{10-x}Cu_x(PO_4)_6O$ at $x \approx 1$ is dominated predominately by Cu bands, the precise arrangement of the Cu atoms and hence the lattice formed by these very Cu atoms is more difficult to predict in DFT. Periodically extending the single unit cells results in a triangular arrangement of the Cu-atoms (blue) in Fig. 1(b). Other arrangements of the Cu atoms on the Pb(1) sites are possible and have not been studied. They will result, because of the rather larger Cu-Cu distance, in similarly flat or even flatter bands. In the presence of disorder or for larger supercells, we would expect a similarly small bandwidth but a further suppression of the conductivity. Such a disordered arrangement of the Cu atoms is also unfavorable for long-range superconductivity.

The triangular lattice we find here is highly frustrated regarding magnetic fluctuations. The large distance and thus small hopping between Cu sites further suppresses the strength of prospective magnetic fluctuations. Also the coupling between the layers is weak: the dispersion from Γ to A is about half of that from Γ to M or X in Fig. 2(c). Hence spin fluctuations cannot be expected to be particularly strong' cf. magnetic DFT+U calculations in Sec. III in the Supplemental Material [13].

Discussion: Superconductivity. While we have not performed calculations for superconductivity, we will discuss in the following a possible mechanism on the basis of the electronic structure found, that is, two flat Cu-bands crossing the Fermi energy and two somewhat more dispersive O bands immediately below. In contrast to cuprates, the small hopping and lattice frustration suppress antiferromagnetic spin fluctuations. This speaks strongly against spin-fluctuation as the pairing glue at elevated temperatures. Ferromagnetism, on the other hand, is known to prevail in flat bands [19]: As U dominates over W, the cost in kinetic energy for a ferromagnetic arrangement becomes small compared to the energy gained by avoiding the Coulomb energy in a fully polarized ferromagnet.

Similarly, and competing with ferromagnetic order, superconductivity can arise from flat bands [20–22]. This flat-band mechanism is discussed, among others, as a possible mechanism for superconductivity in flat moiré bands [23,24]. It is not at all clear, however, whether the band structure of $Pb_9Cu(PO_4)_6O$ provides for the ideal combination of flat and dispersive bands [20,22]. With the bands labeled 1,2 and 3,4 in Fig. 2(c), we have at least the necessary ingredients.

Another possibility, as already discussed in [9], is the complicated interplay between strong electronic correlations and the BCS electron-phonon mechanism. Indeed, this scenario with an increase of T_C due to the enhanced quasiparticle density of states was advocated in [9], in which it was coined the Brinkman-Rice-BCS mechanism [25]. This scenario is somewhat hampered by the fact that also the pairing interaction gets reduced by the quasiparticle renormalization. Nonetheless, an enhancement of superconductivity by electronic correlations is possible [26]. While we have not calculated the electron-phonon coupling, our DFT results attest to an extraordinarily sharp peak at the Fermi energy, which is expected to be even further narrowed through such quasiparticle renormalization for the doped Mott or charge-transfer insulator. Hence both of the above scenarios for superconductivity are conceivable.

Scenarios of one-dimensional superconductivity [9] and tunneling between two-dimensional semiconductor quantum wells [8] have also been proposed. This is not supported by the rather similar dispersion of the low-energy Cu d-bands in and out of plane in Fig. 2(c). Only the extra O bands 3,4 below the Fermi energy with a large Γ-A dispersion could be considered to be one-dimensional in a first approximation.

What can we learn from our DFT calculations for prospective nonsuperconducting explanations of the experimental results of $Pb_9Cu(PO_4)_6O$ [7–9]? The sharp drop in resistivity might also occur from an ordering or structural transition, possibly affecting the lattice of the Cu dopants (at least when seeking to explain the low-T resistivity of the noise level [7,9], not the 10^{-10}–10^{-11} Ω cm stated in [8]). The putative Meißner effect and negative susceptibility could also result from a diamagnetic state. Here, however, our calculations provide some evidence against such a scenario. The narrow band(s) and the Cu $3d^9$ electronic configuration indicate an (only slightly) screened spin-$\frac{1}{2}$. A strong paramagnetic response can thus be expected. It is difficult to imagine how this can be overcome by a diamagnetic orbital response.

Conclusion. Our DFT calculations and consideration regarding correlation effects put $Pb_9Cu(PO_4)_6O$ in an ultra-strongly-correlated regime, with U/W of $O(10)$ instead of $O(1)$ in cuprate superconductors because of the very narrow Cu band(s) crossing the Fermi energy. In such a situation, the Coulomb interaction U clearly dominates over the kinetic energy and bandwidth W. This can give rise to flat-band superconductivity or a correlation-enhanced BCS mechanism. A strong diamagnetic response, on the other hand, is not expected.

It is a bit puzzling why $Pb_{10-x}Cu_x(PO_4)_6O$ with such a large U/W was not a Mott insulator or charge transfer insulator in experiment. A possible explanation is hole or electron doping through some off-stoichiometry (different from x) in experiment. Such an additional doping would put $Pb_{10-x}Cu_x(PO_4)_6O$ into the class of doped Mott or charge-transfer insulators. Note that Pb and Cu are both 2+, hence other dopings x will not change the Cu^{2+} oxidation state; $Pb_{10-x}Cu_x(PO_4)_6O$ remains insulating for all x. This puts O (or P) deficiency or excess as a possible source for such an accidental doping off-stoichiometry. Given the synthesis procedure [9], the replacement of O or P by S is also conceivable. Against this background, it might be advisable to actively procure such a doping in the synthesis process, e.g., by controlling the O partial pressure or adding small amounts of a reducing or oxidizing agent.

Note added. Independently to our work, three other DFT studies appeared simultaneously on arXiv [27–29] but did not conclude $Pb_9Cu_1(PO_4)_6O$ to be insulating. The insulating nature of $Pb_{10}(PO_4)_6O$, on the other hand, is already apparent in DFT, and it has also been discussed in [27,28,30]. The Mott or charge-transfer insulating state of $Pb_9Cu_1(PO_4)_6O$ has been confirmed in subsequent theoretical calculations [31–35] and experiment [36–40]. While we considered here that unintended doping leads to (super)conductivity in LK-99, a plausible alternative explanation is that the observed conductivity jumps are caused by residual Cu_2S in the sample [39,41,42].

Acknowledgments. We acknowledge funding through the Austrian Science Funds (FWF) projects I 5398, P 36213, SFB Q-M&S (FWF project ID F86), and Research Unit QUAST by the Deutsche Forschungsgemeinschaft (DFG; project ID

FOR5249) and FWF (project ID I 5868). L.S. is thankful for the starting funds from Northwest University. Calculations have been done on the Vienna Scientific Cluster (VSC) and supercomputing clusters at Northwest University.

[1] J. Bardeen, L. N. Cooper, and J. R. Schrieffer, Phys. Rev. **106**, 162 (1957).

[2] J. G. Bednorz and K. A. Müller, Z. Phys. B **64**, 189 (1986).

[3] A. P. Drodzov, M. I. Eremets, I. A. Troyan, V. Ksenofontov, and S. I. Shylin, Nature (London) **525**, 73 (2015).

[4] D. Li, K. Lee, B. Y. Wang, M. Osada, S. Crossley, H. R. Lee, Y. Cui, Y. Hikita, and H. Y. Hwang, Nature (London) **572**, 624 (2019).

[5] S. Zeng, C. S. Tang, X. Yin, C. Li, M. Li, Z. Huang, J. Hu, W. Liu, G. J. Omar, H. Jani, Z. S. Lim, K. Han, D. Wan, P. Yang, S. J. Pennycook, A. T. S. Wee, and A. Ariando, Phys. Rev. Lett. **125**, 147003 (2020).

[6] D. Li, B. Y. Wang, K. Lee, S. P. Harvey, M. Osada, B. H. Goodge, L. F. Kourkoutis, and H. Y. Hwang, Phys. Rev. Lett. **125**, 027001 (2020).

[7] S. Lee, J. Kim, S. Im, S. An, Y.-W. Kwon, and K. H. Auh, J. Kor. Cryst. Growth Cryst. Technol. **33**, 61 (2023).

[8] S. Lee, J.-H. Kim, and Y.-W. Kwon, arXiv:2307.12008.

[9] S. Lee, J. Kim, H.-T. Kim, S. Im, S. An, and K. H. Auh, arXiv:2307.12037.

[10] G. Kresse and J. Hafner, Phys. Rev. B **47**, 558 (1993).

[11] G. Kresse and J. Furthmüller, Comput. Mater. Sci. **6**, 15 (1996).

[12] J. P. Perdew, A. Ruzsinszky, G. I. Csonka, O. A. Vydrov, G. E. Scuseria, L. A. Constantin, X. Zhou, and K. Burke, Phys. Rev. Lett. **100**, 136406 (2008).

[13] See Supplemental Material at http://link.aps.org/supplemental/10.1103/PhysRevB.108.L121110 for information regarding additional DFT and DFT+U results. This includes references to K. Schwarz, P. Blaha, and G. K. H. Madsen, Comput. Phys. Commun. **147**, 71 (2002); A. A. Mostofi, J. R. Yates, Y.-S. Lee, I. Souza, D. Vanderbilt, and N. Marzari, *ibid.* **178**, 685 (2008); J. Kunes, R. Arita, P. Wissgott, A. Toschi, H. Ikeda, and K. Held, *ibid.* **181**, 1888 (2010); A. I. Liechtenstein, V. I. Anisimov, and J. Zaanen, Phys. Rev. B **52**, R5467 (1995); H. Eskes and G. A. Sawatzky, Phys. Rev. Lett. **61**, 1415 (1988); G. H. Wannier, Phys. Rev. **52**, 191 (1937); N. Marzari, A. A. Mostofi, J. R. Yates, I. Souza, and D. Vanderbilt, Rev. Mod. Phys. **84**, 1419 (2012).

[14] S. V. Krivovichev and P. C. Burns, Z. Kristallogr.-Cryst. Mater. **218**, 357 (2003).

[15] S.-L. Yang, J. A. Sobota, Y. He, Y. Wang, D. Leuenberger, H. Soifer, M. Hashimoto, D. H. Lu, H. Eisaki, B. Moritz, T. P. Devereaux, P. S. Kirchmann, and Z.-X. Shen, Phys. Rev. B **96**, 245112 (2017).

[16] P. Worm, M. Kitatani, J. M. Tomczak, L. Si, and K. Held, Phys. Rev. B **105**, 085110 (2022).

[17] G. Kotliar, S. Y. Savrasov, K. Haule, V. S. Oudovenko, O. Parcollet, and C. A. Marianetti, Rev. Mod. Phys. **78**, 865 (2006).

[18] K. Held, Adv. Phys. **56**, 829 (2007).

[19] A. Mielke and H. Tasaki, Commun. Math. Phys. **158**, 341 (1993).

[20] K. Kuroki, T. Higashida, and R. Arita, Phys. Rev. B **72**, 212509 (2005).

[21] V. I. Iglovikov, F. Hébert, B. Grémaud, G. G. Batrouni, and R. T. Scalettar, Phys. Rev. B **90**, 094506 (2014).

[22] H. Aoki, J. Supercond. Nov. Magn. **33**, 2341 (2020).

[23] Y. Cao, V. Fatemi, S. Fang, K. Watanabe, T. Taniguchi, E. Kaxiras, and P. Jarillo-Herrero, Nature (London) **556**, 43 (2018).

[24] L. Balents, C. R. Dean, D. K. Efetov, and A. Young, Nat. Phys. **16**, 725 (2020).

[25] H. T. Kim, Sci. Rep. **11**, 10329 (2021).

[26] M. Capone, M. Fabrizio, C. Castellani, and E. Tosatti, Science **296**, 2364 (2002).

[27] J. Lai, J. Li, P. Liu, Y. Sun, and X.-Q. Chen, J. Mater. Sci. Technol. **171**, 66 (2024).

[28] R. Kurleto, S. Lany, D. Pashov, S. Acharya, M. van Schilfgaarde, and D. S. Dessau, arXiv:2308.00698.

[29] J. Cabezas-Escares, N. Barrera, C. Cardenas, and F. Munoz, arXiv:2308.01135.

[30] S. Yang, G. Liu, and Y. Zhong, arXiv:2308.13938.

[31] L. Si, M. Wallerberger, A. Smolyanyuk, S. di Cataldo, J. M. Tomczak, and K. Held, arXiv:2308.04427.

[32] D. M. Korotin, D. Y. Novoselov, A. O. Shorikov, V. I. Anisimov, and A. R. Oganov, arXiv:2308.04301.

[33] C. Yue, V. Christiansson, and P. Werner, arXiv:2308.04976.

[34] J. Liu, T. Yu, J. Li, J. Wang, J. Lai, Y. Sun, X.-Q. Chen, and P. Liu, arXiv:2308.11766.

[35] A. B. Georgescu, arXiv:2308.07295.

[36] K. Kumar, N. Karn, Y. Kumar, and V. Awana, arXiv:2308.03544.

[37] P. Puphal, M. Akbar, M. Hepting, E. Goering, M. Isobe, A. Nugroho, and B. Keimer, arXiv:2308.06256.

[38] Y. Jiang, S. B. Lee, J. Herzog-Arbeitman, J. Yu, X. Feng, H. Hu, D. Călugăru, P. S. Brodale, E. L. Gormley, M. G. Vergniory *et al.*, arXiv:2308.05143.

[39] C. Liu, W. Cheng, X. Zhang, J. Xu, J. Li, Q. Shi, C. Yuan, L. Xu, H. Zhou, S. Zhu, J. Sun, W. Wu, J. Luo, K. Jin, and Y. Li, Phys. Rev. Mater. **7**, 084804 (2023).

[40] P. Wang, X. Liu, J. Ge, C. Ji, H. Ji, Y. Liu, Y. Ai, G. Ma, S. Qi, and J. Wang, Quantum Frontiers **2**, 10 (2023).

[41] S. Zhu, W. Wu, Z. Li, and J. Luo, arXiv:2308.04353.

[42] P. K. Jain, arXiv:2308.05222 [J. Phys. Chem C (to be published), doi: 10.1021/acs.jpcc.3c05684].